On the Analysis of Resonators Using Finite-Difference Time-Domain Techniques

Christopher L. Wagner and John B. Schneider

***Abstract*—Because a resonator with perfect electrically conducting (PEC) walls has no complications with absorbing boundary conditions and, for canonical geometries, the resonant frequencies are trivial to find, resonators are often used for analyzing the performance of finite-difference time-domain (FDTD) methods. However, when testing the performance of boundary implementations in an FDTD scheme, one should compare to the resonant frequencies of a "perfect" discretized resonator (not to the mode frequencies in the continuous world). On the other hand, when testing the dispersion properties of a method, the resonant frequencies for some structures can be obtained directly from the dispersion relation, thus obviating the need for any simulation. Here, we demonstrate how the dispersion relation can be used to obtain *all* the resonant frequencies of a rectangular resonator modeled with the Yee algorithm. Furthermore, it is shown that modes that are degenerate in the continuous world can split into distinct modes in FDTD resonators, while modes that are separate in the continuous world can combine in FDTD resonators, thus yielding extra or missing modes. Analytic results are verified using numerical simulations.**

***Index Terms*—Finite-difference time-domain (FDTD).**

I. Introduction

CANONICAL resonators have been used to quantify the performance of finite-difference time-domain (FDTD) methods designed to model boundaries that are not aligned with the grid (e.g., [1] and [2]). Resonators or resonant-like structures have also been used in simulations to demonstrate the dispersion properties of a scheme (e.g., [3] or [4], where a parallel plate waveguide was used). When the goal is to ascertain the quality of the implementation of boundary conditions (such as the use of a locally conformal scheme to realize a PEC boundary), one should try to separate the errors introduced by inherent grid dispersion from those introduced by the boundary conditions themselves. To accomplish this, the resonant frequencies obtained in a simulation should be compared not to frequencies of the corresponding resonator in the continuous world, but rather to the frequencies of a "perfect" discretized scatterer, i.e., one that suffers the inherent anisotropy and dispersion of the grid, but does not have any boundary errors. We show that the dispersion relation for the Yee algorithm can be used to predict precisely the frequencies at which modes will oscillate in a rectangular resonator. Due to the anisotropic dispersion of the Yee algorithm, modes that have degenerate frequencies in the continuous world may split into distinct frequencies in the discretized world. Conversely, other modes that one would anticipate are distinct may combine in an FDTD simulation. Given the ability to obtain the resonant behavior of some structures directly from the dispersion relation, it seems unnecessary to perform simulations using a resonator to quantify the dispersion properties of a given method. These simulations yield no insight into the method that is not already implicitly contained in the dispersion relation itself.

We start by reviewing the Yee dispersion relation. We then show how it can be used to predict the resonances that will be present in a rectangular structure. Mode shifting, splitting, and combining are illustrated with simulations and with use of a frequency-versus-wavenumber diagram.

The Yee dispersion relation, in rectangular coordinates, is given by [5]

$$\left(\frac{1}{c\Delta t}\sin\frac{\tilde{\omega}\Delta t}{2}\right)^2=\left(\frac{1}{\Delta x}\sin\frac{k_x\Delta x}{2}\right)^2+\left(\frac{1}{\Delta y}\sin\frac{k_y\Delta y}{2}\right)^2+\left(\frac{1}{\Delta z}\sin\frac{k_z\Delta z}{2}\right)^2 \quad (1)$$

where Δt is the time step, $\tilde{\omega}$ is the numeric frequency, k_x, k_y, and k_z are the wavenumber components, and Δx, Δy, and Δz are the cell lengths in the respective directions. For cubic cells, this reduces to

$$\frac{1}{S^2}\sin^2\left(\frac{\tilde{\omega}\Delta t}{2}\right)=\sin^2\left(\frac{k_x\delta}{2}\right)+\sin^2\left(\frac{k_y\delta}{2}\right)+\sin^2\left(\frac{k_z\delta}{2}\right) \quad (2)$$

where S is the Courant number equal to $c\Delta t/\delta$, and δ is the cell length. Note, that the resonant wavenumbers are dictated by the physical size of the structure and this can be controlled precisely in the FDTD simulation. Thus, the wavenumbers in the continuous and discrete worlds correspond exactly. However, the frequencies that gives rise to those wavenumbers differ.

A resonator with PEC walls has resonant mode frequencies given by

$$\omega^2=(\pi c)^2\left[\left(\frac{m}{L_x}\right)^2+\left(\frac{n}{L_y}\right)^2+\left(\frac{p}{L_z}\right)^2\right] \quad (3)$$

where m, n, and p are the mode indices, and L_x, L_y, and L_z are the size of the resonator in the x, y, and z directions, respectively. In terms of the wavenumber components, (3) can be written as follows:

$$\omega^2=c^2\left(k_x^2+k_y^2+k_z^2\right). \quad (4)$$

Manuscript received March 23, 2001; revised November 6, 2002.

The authors are with the School of Electrical Engineering and Computer Science, Washington State University, Pullman, WA 99164-2752 USA (e-mail: clwagner@eecs.wsu.edu; schneidj@eecs.wsu.edu).

Digital Object Identifier 10.1109/TAP.2003.817572

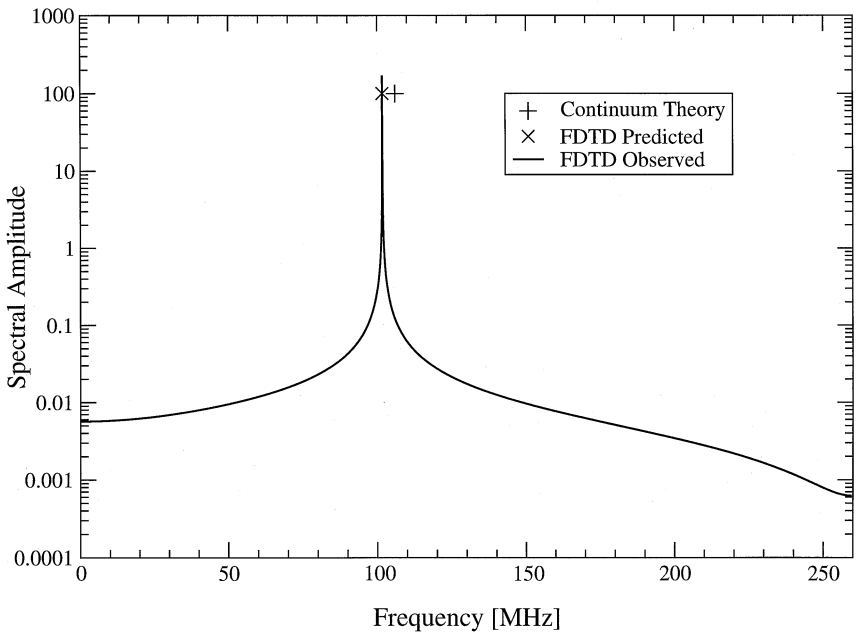

Fig. 1. Continuum and predicted resonant frequencies as well as observed spectrum for a $2 \times 2 \times 1$ resonator. Continuum and FDTD predicted frequencies are indicated with symbols drawn with arbitrary amplitudes.

That is, given the mode indices, the corresponding wavenumbers are given by

$$k_x = \frac{m\pi}{L_x}, \qquad k_y = \frac{n\pi}{L_y}, \qquad k_z = \frac{p\pi}{L_z}. \tag{5}$$

Putting (2) and (5) together, and solving for $\tilde{f} = \tilde{\omega}/2\pi$, we obtain the following:

$$\tilde{f} = \frac{1}{\pi\Delta t}\sin^{-1} \times \left(S\sqrt{\left(\sin\frac{m\pi\delta}{2L_x}\right)^2 + \left(\sin\frac{n\pi\delta}{2L_y}\right)^2 + \left(\sin\frac{p\pi\delta}{2L_z}\right)^2} \right). \tag{6}$$

This gives the resonant frequency $\tilde{f}$ for a particular set of mode indices for any FDTD rectangular resonator. When a resonator has the same size in more than one dimension, modes with permutations of indices will be degenerate. For example, if $L_x = L_y$, modes (1,7,0) and (7,1,0) are degenerate. When a mode has this type of degeneracy we will refer to the mode in the plural even if a single set of indices is given.

In the continuum, any resonator has an infinite number of modes. In a discrete space there will be a finite number due to the spatial sampling of the grid. The highest frequency that may be coupled into the grid, i.e., the grid Nyquist frequency, is $1/2\Delta t$ [6]. In the continuum, there are modes whose frequencies are below the grid Nyquist frequency but that have wavenumber components that are complex [6], [7]. The transition between purely real and complex wavenumbers occurs where there are exactly two grid points per numeric wavelength. Complex wavenumber components experience exponential decay, and hence, the corresponding mode does not resonate. Therefore, the continuum theory is applied here with the understanding that the wavenumbers do not extend beyond those that are real in the FDTD grid. From (6), it appears that one can use any value for the mode indices and still obtain a real result (assuming S is less than the stability limit of $1/\sqrt{3}$). This is true of this equation, but that observation masks, to some extent, the true behavior of the grid and what is realizable. Regardless of the direction of propagation, there must be at least two samples per numeric wavelength, i.e., the minimum wavelength $\lambda_{\min}$, is 2δ. The wavenumber corresponding to this discretization is $k_{\max} = 2\pi/\lambda_{\min} = \pi/\delta$. Using this as a bound on a single wavenumber component, say the k_x component, and equating with the expression given in (5), we obtain $k_x = m\pi/L_x \leq \pi/\delta$. This places a bound on the mode index m such that $m \leq L_x/\delta$. Therefore, if the resonator size L_x is N cells, then m can be no larger than N. Similar arguments hold in the other directions.

II. FDTD Simulations

Here, we demonstrate the agreement of measured and predicted values for FDTD resonators. The rectangular resonators are excited by a single element current source in the z direction, centered in the domain. The source is a unit amplitude current of duration $2\Delta t$, giving a spectral null at the grid Nyquist frequency. The z component of the electric field is sampled at the location of the source. This data is Fourier transformed to produce the mode spectral plots shown below. With this geometry, the excited and detectable modes will have odd x and y mode indices, while the z axis index will be even. To maintain the source at the center of the domain, there must be an even number of cells in the x and y directions and an odd number in the z direction. For simplicity, the domain is kept as nearly cubic as possible so the number of cells in the z direction is one less than in x and y. Unit cells are cubic, with E fields along the cell edges. Without loss of generality, unit cells are assigned a size of $\delta = 1$ m. The simulations use the Courant limit ($1/\sqrt{3}$) and are run for 65 536 time steps. An FFT was

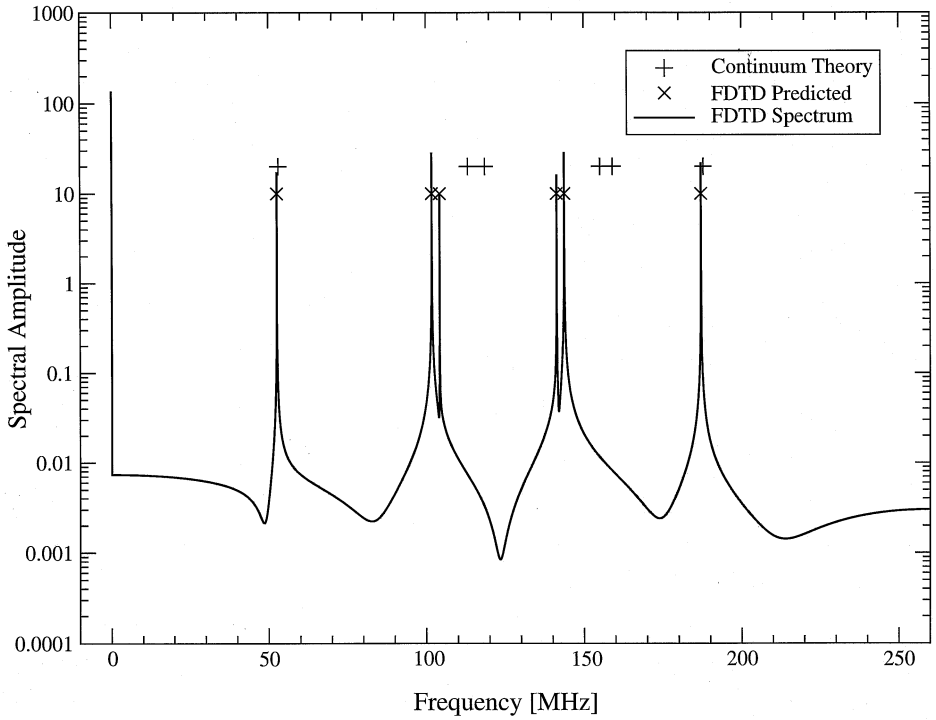

Fig. 2. Continuum and FDTD predicted resonant frequencies as well as observed spectrum for a $4 \times 4 \times 3$ resonator. Note the good performance of the FDTD method for the highest frequency mode. This mode is (3,3,2) which is almost along the major diagonal. Continuum and FDTD predicted frequencies are plotted with arbitrary amplitude.

used to obtain spectral information. Using these parameters, the Nyquist frequency is 259.6278 MHz and the spectral resolution Δf is 7.923 211 kHz. In the spectral plots to follow, symbols are used to designate continuum and FDTD predicted resonant frequencies while a line shows the result of the FDTD simulation (i.e., a solid line shows the entire spectrum obtained from the simulation). Specifically, plus signs are used to indicate the continuum frequencies obtained via (3), while X's are used to indicate FDTD frequencies obtained via (6).

The difference between the continuum resonance and the FDTD resonance, as well as the ability to predict the FDTD resonant frequency, can be demonstrated with a trivially small resonator. The smallest possible resonator with the geometry described above has a volume of $2 \times 2 \times 1$ cells. Such a resonator has only one mode, the (1,1,0) mode. The continuum frequency is 105.9927 MHz. Equation (6) predicts the FDTD frequency will be 101.7291 MHz, and this agrees within $\pm\Delta f$ of the observed FDTD results, as shown in Fig. 1.

To illustrate more clearly nonlinear effects, a resonator with a size of $4 \times 4 \times 3$ is considered next. The amplitude spectrum is shown in Fig. 2. Note that the FDTD predicted values match the observed spectral peaks, whereas the continuum frequencies do not. The (1,3,0) modes are dispersion shifted to a frequency lower than the (1,1,2) mode, and the (3,3,0) mode is shifted to below the (1,3,2) modes as shown in Table I. There is a large dc line [8] due to the charge deposited by the pulsed source. A dc line does not exist for the previous resonator because that small resonator did not provide ample room to store charge to either side of the source (i.e., the charge was effectively shorted by the walls of the resonator).

TABLE I
$4 \times 4 \times 3$ RESONATOR FREQUENCIES. THE OBSERVED FREQUENCIES ARE WITHIN $\pm\Delta f$ OF THE PREDICTED VALUES. ALL FREQUENCIES ARE IN MEGAHERTZ

Mode	Continuum Theory	FDTD Predicted	FDTD Observed
$(1,1,0)$	52.99633	52.52425	52.52297
$(1,1,2)$	113.1140	104.2227	104.2219
$(1,3,0)$	118.5034	101.7291	101.7261
$(1,3,2)$	155.0136	143.6522	143.6557
$(3,3,0)$	158.9890	141.2610	141.2629
$(3,3,2)$	187.7862	187.0015	187.0036

In Fig. 2, note the relatively good agreement between the FDTD resonance and the continuum theory at the highest resonant frequency. This is, at first, somewhat counter-intuitive since this resonance occurs in a region with coarse discretization where one might expect the worst dispersion errors. However, this peak corresponds to the (3,3,2) mode whose associated wavevectors are nearly aligned with the grid diagonals. Since these simulations are run at the Courant limit, there is no grid dispersion along the grid diagonals regardless of the discretization. This illustrates that, due to the anisotropy of the grid, the amount of dispersion is a function of both the discretization and

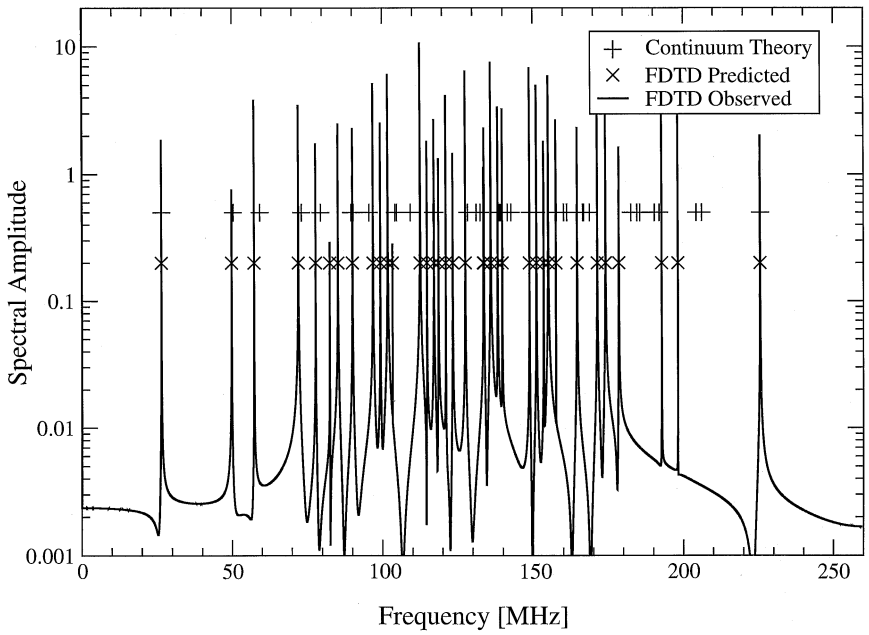

Fig. 3. Continuum and FDTD predicted resonant frequencies as well as observed spectrum for an $8 \times 8 \times 7$ resonator. Continuum and FDTD predicted frequencies are plotted with arbitrary amplitude. The dc line is not shown.

the direction of propagation. For a general resonator in which one does not know the orientation of the associated wavevectors, one would be unable to say if the agreement between the FDTD-generated resonances and the continuum resonances are getting better or worse as the frequency increases. Nevertheless, one can be confident that agreement is good for well-resolved frequencies (i.e., ones for which the discretization is high enough to ensure low dispersion for all directions of propagation).

Mode splitting is a result of the anisotropic dispersion of the Yee grid. Modes with the same continuum frequency can have different dispersion shifts owing to their different wavenumber components. This occurs because continuum degenerate modes having distinct sets of indices suffer different dispersion in the FDTD grid, thus resulting in two (or more) spectral lines. The smallest resonator where splitting occurs is the $8 \times 8 \times 7$ resonator. For example the (1,7,0) and the (5,5,0) modes are degenerate. However, the dispersion shift will be different for the (1,7,0) modes and (5,5,0) mode, thus splitting this line. The same thing occurs if the third index is 2, 4, or 6. The measured and predicted resonances for the $8 \times 8 \times 7$ resonator are shown in Fig. 3. Again, there is perfect agreement between the predicted and measured FDTD frequencies, and these frequencies may differ substantially from the continuum frequency.

The resonators illustrated here do not exhibit an extra total number of mode lines since some modes also combine while others split. However, once the size of the resonator is above $20 \times 20 \times 19$, the FDTD resonator will have more mode lines than the continuum theory predicts.

Mode combining occurs when two (or more) distinct modes suffer different dispersion resulting in the lines combining to form a single line. In the case of the $8 \times 8 \times 7$ resonator, the (1,7,0) modes are dispersion shifted to the same frequency as the dispersion-shifted (3,5,0) mode, thus yielding a single spectral line in the simulation.

The mechanics of mode splitting and combining is perhaps best understood using an f-k (ω-β) diagram of the frequency versus the wavenumber. Fig. 4 shows such a diagram that can be used to demonstrate the splitting and combining of the modes mentioned above. First, one draws a straight line of slope $c/2\pi$ representing the relationship between frequency and wavenumber magnitude in the continuum. Assume one is interested in the (1,7,0) and (5,5,0) modes which are degenerate in the continuum. The dispersion curves for these modes are added to the plot. To generate these curves, the magnitude of the wavenumber is now treated as the independent variable. For the (1,7,0) mode, one plots

$$\frac{1}{S^2}\sin^2\left(\frac{2\pi f\Delta t}{2}\right) = \sin^2\left(\frac{k\delta}{2\sqrt{50}}\right) + \sin^2\left(\frac{7k\delta}{2\sqrt{50}}\right) \quad (7)$$

while for the (5,5,0) mode, one plots

$$\frac{1}{S^2}\sin^2\left(\frac{2\pi f\Delta t}{2}\right) = 2\sin^2\left(\frac{5k\delta}{2\sqrt{50}}\right). \quad (8)$$

Now, (3) is used to obtain the continuum frequency for the resonant mode. This point is identified in Fig. 4 by the intersection of the straight continuum line and the horizontal line labeled "Continuum (1,7,0) & (5,5,0)." Since the FDTD resonator must have the same wavenumbers, one draws a vertical line from that point on the continuum line and finds the intersections with the dispersion curves for the (1,7,0) and (5,5,0) modes. These intersections are indicated with the horizontal lines labeled "Observed (5,5,0)" and "Observed (1,7,0)." The vertical distance between these horizontal lines shows the difference in frequency of these supposedly degenerate modes.

Mode combining is illustrated in a similar fashion. One has to add the dispersion curve for the (3,5,0) mode and identify the

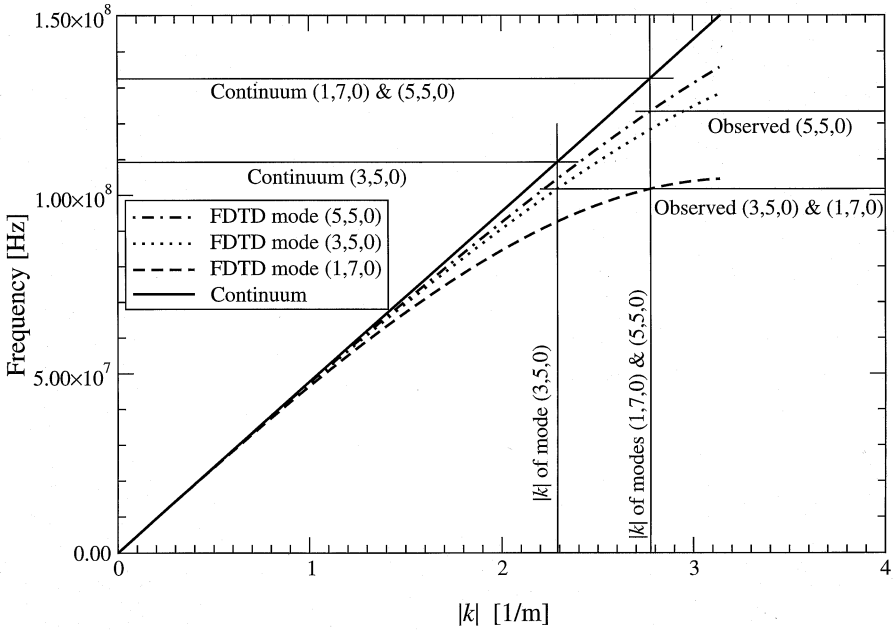

Fig. 4. Dispersion curves (frequency versus wavenumber) for selected modes in the $8 \times 8 \times 7$ resonator, graphically illustrating mode splitting and combining. Horizontal lines labeled "Continuum" are the frequencies which should exist for a given k. Lines labeled "Observed" are the dispersion shifted frequencies that will be seen in the FDTD simulation.

TABLE II
SELECTED LIST OF $8 \times 8 \times 7$ RESONATOR MODE FREQUENCIES, SHOWING THE EFFECT OF COMBINING AND SPLITTING. THE (1,7,0) MODE SPLIT FROM THE (5,5,0) MODE AND COMBINES WITH THE (3,5,0) MODE, JUMPING OVER INTERVENING MODES. SIMILAR SPLITTING/COMBINING OCCURS WITH A THIRD INDEX OF 2, 4, OR 6. OBSERVED DEGENERATE MODES CANNOT BE DISTINGUISHED IN THE FDTD DATA. OBSERVED LINE FREQUENCY CLOSEST TO THE PREDICTED LINE IS REPORTED. ALL FREQUENCIES ARE IN MEGAHERTZ

Mode	Continuum Theory	FDTD Predicted	FDTD Observed
$(3,5,0)$	109.2547	101.7291	101.7261
$(3,3,4)$	116.8595	114.7771	114.7756
$(3,5,2)$	117.3490	112.5123	112.5096
$(1,5,4)$	128.3151	121.0187	121.0191
$(1,1,6)$	131.1865	103.2788	103.2791
$(1,7,0)$	132.4908	101.7291	101.7261
$(5,5,0)$	132.4908	123.3438	123.3406

frequency for the corresponding continuum resonance. Drawing a vertical line from that point on the continuum line, one finds that the intersection with the (3,5,0) dispersion curve is precisely at the same frequency as the (1,7,0) mode. Hence, these distinct modes in the continuum yield a single resonance in the FDTD simulation. The frequencies associated with these modes are given in Table II.

III. CONCLUSION

The dispersion relation accurately predicts the frequencies at which a rectangular resonator mode will resonate. Dispersion can split or combine modes. Furthermore, the dispersion shift can change the resonant frequencies so that a list of observed modes ordered by resonant frequency may or may not correspond in order to a list obtained from the continuum.

The Yee dispersion anisotropy is responsible for mode splitting and combining. Algorithms which are more isotropic than Yee, such as the Forgy isotropic scheme [9] which is isotropic to fourth order, will have reduced mode splitting. Given the dispersion relation one can post-process resonance data to correct for the mean dispersion error. Such a correction would shift peaks but would not undo any splitting or combining.

The resonant analysis conducted here was limited to the Yee scheme, but a similar analysis can be conducted for any FDTD scheme for which a dispersion relation exists. It is to be noted that the rectangular resonators considered here have simple resonances in which the fields can be viewed as the superposition of plane waves propagating in discrete directions. Knowing the directions and the corresponding frequencies, and given the dispersion relation, one can exactly predict the amount of error in the resonant frequency obtained from a simulation. However, for a general resonator in which the wavevectors associated with a given mode are not known one cannot determine the amount of error, nor can one completely correct for that error, unless the particular scheme has the same amount of error for all wavevectors at a given discretization. The Yee scheme, which is anisotropic to second order, permits only limited correction where one can correct for the mean dispersion error. Such a technique is essentially the one applied in the dispersion correction technique described by Nehrbass *et al.* [10] (however, they

applied the correction at a single frequency prior to the simulation rather than as a post-processing correction across all frequencies). On the other hand, correcting for the mean dispersion error in the Forgy scheme (which is, same as the Yee algorithm, second-order accurate but, unlike the Yee algorithm, isotropic to fourth order) would yield results that are more accurate than those which could be obtained from the (corrected) Yee algorithm at the same discretization.

REFERENCES

[1] S. Dey and R. Mittra, "A locally conformal finite-difference time-domain (FDTD) algorithm for modeling three-dimensional perfectly conducting objects," *IEEE Microwave Guided Wave Lett.*, vol. 7, pp. 273–275, Sept. 1997.

[2] C. J. Railton and J. B. Schneider, "An analytical and numerical analysis of several locally conformal FDTD schemes," *IEEE Trans. Microwave Theory Tech.*, vol. 47, pp. 56–66, Jan. 1999.

[3] M. Fujii and W. J. R. Hoefer, "Application of biorthogonal interpolating wavelets to the Galerkin scheme of time dependent Maxwell's equations," *IEEE Microwave Guided Wave Lett.*, vol. 11, pp. 22–24, Jan. 2001.

[4] J. L. Young, "The design of high-order, leap-frog integrators for Maxwell's equations," in *Proc. IEEE Antennas Propagation Soc. Int. Symp.*, vol. 1, Orlando, FL, July 1999, pp. 176–179.

[5] A. Taflove and M. E. Brodwin, "Numerical solutioin of steady-state electromagnetic scattering problems using the time-dependant Maxwell's equations," *IEEE Trans. Microwave Theory Tech.*, vol. MTT-23, pp. 623–630, Aug. 1975.

[6] J. B. Schneider and R. J. Kruhlak, "Dispersion of homogenous and inhomogenous waves in the Yee finite-difference time-domain grid," *IEEE Trans. Microwave Theory Tech.*, vol. 49, pp. 280–287, Feb. 2001.

[7] J. B. Schneider and C. L. Wagner, "FDTD dispersion revisited: Faster-than-light propagation," *IEEE Trans. Microwave Theory Tech.*, vol. 9, pp. 54–56, Feb. 1999.

[8] C. L. Wagner and J. B. Schneider, "Divergent fields, charge, and capacitance in FDTD simuilations," *IEEE Trans. Microwave Theory Tech.*, vol. 46, pp. 2131–2136, Dec. 1998.

[9] E. A. Forgy and W. C. Chew, "A time-domain method with isotropic dispersion and increased stability on an overlapped lattice," *IEEE Trans. Antennas Propagat.*, vol. 50, pp. 983–996, July 2002.

[10] J. W. Nehrbass, J. O. Jevtić, and R. Lee, "Reducing the phase error for finite-difference methods without increasing the order," *IEEE Trans. Antennas Propagat.*, vol. 46, pp. 1194–2401, Aug. 1998.

Christopher L. Wagner received the B.S. degree in physics and the B.S.E.E. degree from the University of Washington, Seattle, in 1979 and the M.S.E.E degree from Washington State University, Pullman, in 1998.

Previously, he worked as a Research Engineer for SAIC, Bellevue, WA, and recently as a Consultant for International Sensor Technology. Currently, he conducts research in computational electromagnetics and acoustics at the School of Electrical Engineering and Computer Science, Washington State University.

John B. Schneider received the B.S. degree in electrical engineering from Tulane University, New Orleans, LA, and the M.S. and Ph.D. degrees in electrical engineering from the University of Washington, Seattle.

He is presently an Associate Professor at the School of Electrical Engineering and Computer Science, Washington State University, Pullman. His research interests include the use of computational methods to analyze acoustic, elastic, and electromagnetic wave propagation.